

Spatial inhomogeneity and strong correlation physics: a dynamical mean field study of a model Mott-insulator/band-insulator heterostructure

Satoshi Okamoto and Andrew J. Millis

Department of Physics, Columbia University, 538 West 120th Street, New York, New York 10027, USA

(Dated: July 5, 2018)

We use the dynamical mean field method to investigate electronic properties of heterostructures in which finite number of Mott-insulator layers are embedded in a spatially infinite band-insulator. The evolution of the correlation effects with the number of Mott insulating layers and with position in the heterostructure is determined, and the optical conductivity is computed. It is shown that the heterostructures are generally metallic, with moderately renormalized bands of quasiparticles appearing at the interface between the correlated and uncorrelated regions.

PACS numbers: 73.21.-b, 71.27.+a, 73.40.-c, 78.20.-e

An exciting new direction in materials science is the fabrication and study of heterostructure involving “correlated electron” materials such as Mott insulators, high-temperature superconductors, and novel magnets[1, 2]. The issues raised by these heterostructures, especially the evolution with position of properties from correlated to uncorrelated, is of fundamental physical interest and would be crucial for prospective devices based on correlated electron compounds. Many interesting systems have been fabricated, including modulation-doped high- T_c superconductors[3, 4], Mott-insulator/band-insulator heterostructures[5], and a variety of combinations of magnetic transition-metal oxides[6, 7, 8], but there has been relatively little theoretical study of the heterostructure-induced changes in many-body physics. The theoretical problem is difficult because it requires methods which can deal both with spatial inhomogeneity and strong correlation physics.

Despite the difficulties, several interesting works have appeared. Fang, Soloviev and Terakura[9] used bulk band structure calculation to gain insight into the effects [6] of strain fields induced by lattice mismatch in a heterostructure. Matzdorf and co-workers used GGA band theory methods to study the surface electronic and lattice structure of Sr_2RuO_4 , predicting a lattice distortion which is observed and surface ferromagnetism which is apparently not observed [10]. Potthoff and Nolting used dynamical-mean-field methods to study the consequences of the lower coordination at a surface [11, 12].

All of these papers, however, treated situations in which the electronic density remained at the bulk value, and the new physics arose from structural differences. A crucial feature of heterostructures is an inhomogeneous electron density caused by a spreading of charge across the interfaces which define the system. Recently [13, 14], we used realistic multi-orbital interaction parameters and a density-functional-theory-derived tight-binding band structure to model ground state properties of the $\text{LaTiO}_3/\text{SrTiO}_3$ heterostructure fabricated by Ohtomo *et al.*[5]. While this study captured important aspects of the density inhomogeneity, it did not address

the dynamical properties of correlated heterostructures. Further, this study employed the Hartree-Fock approximation which is known to be an inadequate representation of strongly correlated materials, and in particular does not include the physics associated with proximity to the Mott insulating state.

In this paper we use the dynamical mean field method [15], which provides a much better representation of the electronic dynamics associated with strong correlations, to study the correlated electron properties of a simple Hubbard-model heterostructure inspired by—but not a fully realistic representation of—the systems studied in [5]. We present results for observables including photoemission spectra, optical conductivity, charge density, and highlight similarities and differences to previous work.

We study a single orbital model with basic Hamiltonian $H_{hub} = H_{band} + H_{int} + H_{coul}$ with

$$H_{band} = -t \sum_{\langle ij \rangle, \sigma} (d_{i\sigma}^\dagger d_{j\sigma} + H.c.), \quad (1)$$

$$H_{int} = U \sum_i n_{i\uparrow} n_{i\downarrow} + \frac{1}{2} \sum_{\substack{i \neq j \\ \sigma, \sigma'}} \frac{e^2 n_{i\sigma} n_{j\sigma'}}{\varepsilon |\vec{R}_i - \vec{R}_j|}. \quad (2)$$

Here the sites i form a simple cubic lattice of lattice constant a , so electronic positions $\vec{R}_i = a(n_i, m_i, l_i)$. We include both an on-site (U) and long ranged Coulomb interaction: the screening field from the latter is important for the electron density profile. We associate the electronic sites with the B-sites of an ABO_3 perovskite lattice, and define the heterostructure by counterions of charge +1 placed on a subset of the A-sites. Here we study an n -layer [001] heterostructure defined by n planes of +1 counterions placed at positions $\vec{R}_j^A = a(n_j + 1/2, m_j + 1/2, l_j + 1/2)$, with $-\infty < n_j, m_j < \infty$ and the l_j running over n adjacent values. The resulting potential is

$$H_{coul} = - \sum_{i,j,\sigma} \frac{e^2 n_{i\sigma}}{\varepsilon |\vec{R}_i - \vec{R}_j^A|}. \quad (3)$$

Charge neutrality requires that the areal density of elec-

trons is n . A dimensionless measure of the strength of the Coulomb interaction is $E_c = e^2/(\varepsilon at)$; we choose parameters somewhat arbitrarily so that $E_c = 0.8$ (this corresponds to $t \sim 0.3$ eV and length $a \sim 4$ Å and $\varepsilon = 15$, which describe the system studied in [5]). We found that the charge profile did not depend in an important way on ε for $5 < \varepsilon < 25$.

The basic object of our study is the electron Green function, which for the [001] heterostructure may be written

$$G(z, z', \vec{k}_{\parallel}; \omega) = [\omega + \mu - H_{band} - H_{Coul} - \Sigma(z, z', \vec{k}_{\parallel}; \omega)]^{-1}. \quad (4)$$

We approximate the self-energy operator as the sum of a Hartree term arising from the long-ranged part of the Coulomb interaction

$$\Sigma_H(z_i) = \sum_{j \neq i, \sigma} \frac{e^2 \langle n_{j\sigma} \rangle}{\varepsilon |\vec{R}_i - \vec{R}_j|} \quad (5)$$

and a dynamical part Σ_D arising from local fluctuations. Following the usual assumptions of dynamical-mean-field theory [15] as generalized to inhomogeneous situations by Schwieger *et. al.* [12], we assume

$$\Sigma_D \Rightarrow \Sigma_D(z, \omega). \quad (6)$$

The layer (z)-dependent dynamical self energy Σ_D is determined from the solution of a quantum impurity model [15] with mean-field function fixed by the self-consistency condition

$$G^{imp}(z, \omega) = \int \frac{d^2 k_{\parallel}}{(2\pi)^2} G(z, z, \vec{k}_{\parallel}; \omega). \quad (7)$$

One must solve a separate impurity model for each layer, but the self consistency condition [cf. Eq. (7)] implies the solutions are coupled. It is also necessary to self-consistently calculate the charge density via $n(z) = -2 \int \frac{d\omega}{\pi} f_{\omega} \text{Im} G^{imp}(z, \omega)$ with f the Fermi distribution function. The numerics are time consuming, and it is therefore necessary to adopt a computationally inexpensive method for solving the quantum impurity models. We use the two-site method of Potthoff [16], which reproduces remarkably accurately the scaling of the quasiparticle weight and lower Hubbard band near the Mott transition. We have also verified [17] that the two site method reproduces within a few percent the $T = 0$ magnetic phase diagram found by Ulmke [18] in a model with an unusual low-energy density of states peak.

Fig. 1 shows the layer-resolved spectral function $A(z, z; \omega) = -\frac{1}{\pi} \int \frac{d^2 k_{\parallel}}{(2\pi)^2} \text{Im} G(z, z, \vec{k}_{\parallel}; \omega + i0^+)$ for a 10-layer heterostructure with $U = 16t$ (about 25% greater than the critical value which drives a Mott transition in a bulk system described by H_{hub} with $n = 1$). The spectral functions are in principle measurable in photoemission or scanning tunneling microscopy. Outside

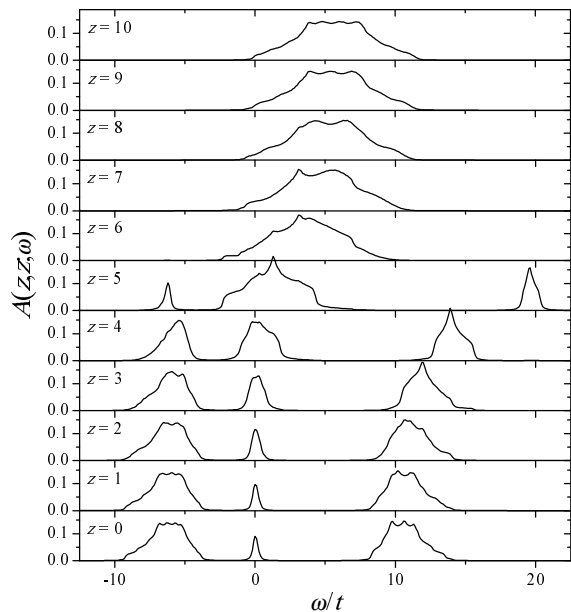


FIG. 1: Layer-resolved spectral function calculated for 10-layer heterostructure for $U = 16t$, $\varepsilon = 15$. The heterostructure is defined by +1 charges placed at $z = \pm 0.5, \pm 1.5, \dots, \pm 4.5$ so the electronic (B) sites are at integer values of z .

the heterostructure ($z > 6$), the spectral function is essentially identical in form to that of the free tight-binding model H_{band} . The electron density is negligible, as can be seen from the fact that almost all of the spectral function lies above the chemical potential. As one approaches the heterostructure ($z = 6$), the spectral function begins to broaden. Inside it ($z \leq 5$) weight around $\omega = 0$ begins to decrease and the characteristic strong correlations structure of lower and upper Hubbard bands with a central quasiparticle peak begins to form. The sharp separation between these features is an artifact of the 2-site DMFT [as is, we suspect, the shift in energy of the upper (empty state) Hubbard band for $z = 4, 5$]. Experience with bulk calculations suggests that the existence of three features and the weight in the quasiparticle region are reliable. Towards the center of the heterostructure, the weight in the quasiparticle band becomes very small, indicating nearly insulating behavior. For very thick heterostructures, we find the weight approaches 0 exponentially.

The behavior shown in Fig. 1 is driven by the variation in density caused by leakage of electrons out of the heterostructure region. Fig. 2 shows the numerical results for the charge-density distribution $n(z)$ for the heterostructure whose photoemission spectra are shown in Fig. 1. One sees that in the center of the heterostructure ($z = 0$) the charge density is approximately 1 per site, and that there exists an edge region, of about three-unit-cell width, over which the density drops from ~ 1 to ~ 0 . The over-all charge profile is determined mainly by the

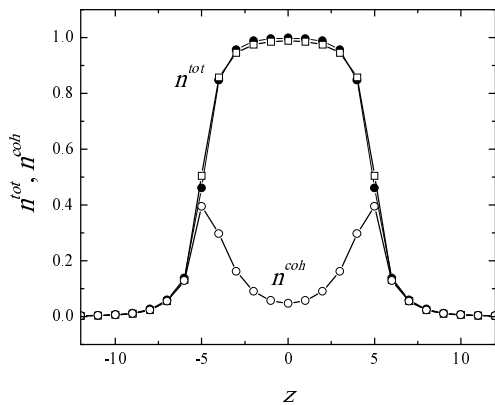


FIG. 2: Total charge density (open squares) and charge density from coherent part near Fermi level (open circles). For comparison, total charge density calculated by applying Hartree Fock approximation to the Hamiltonian shown as filled symbols. Parameters as in Fig. 1.

self consistent screening of the Coulomb fields which define the heterostructure, and is only very weakly affected by the details of the strong on-site correlations (although the fact that the correlations constrain $n < 1$ is obviously important). To show this, we have used the Hartree-Fock approximation to recalculate the charge profile: the results are shown as filled circles in Fig. 2 and are seen to be almost identical to the DMFT results.

The existence of an approximately three unit cell wide edge region where the density deviates significantly from the values $n = 0$ and $n = 1$ characteristic of the two systems in bulk form implies that only relatively thick heterostructures ($n > 6$) will display ‘insulating’ behavior in their central layers, and suggests that the edge regions sustain quasiparticle subbands which give rise to metallic behavior. The open circles in Fig. 2 show the charge density in the ‘quasiparticle bands’ [obtained by integrating $A(z, z; \omega)$ from $\omega = 0$ down to the first point at which $A(z, z; \omega) = 0$]. One sees that these near Fermi-surface states contain a small but non-negligible fraction of the total density, suggesting that edges should display relatively robust metallic behavior. The results represent, a significant correction to the Hartree-Fock calculation [14], which leads, in the edge region, to a metallic quasiparticle density essentially equal to the total density.

The spectral function is determined by the layer-dependent dynamical self-energy $\Sigma_D(z, \omega)$. In bulk materials one distinguishes Fermi liquid and Mott insulators by the low-frequency behavior of Σ_D ; in a Fermi liquid $\Sigma_D \rightarrow_{\omega \rightarrow 0} (1 - Z^{-1})\omega$ (leading to a quasiparticle with renormalized mass) while in a Mott insulator $\Sigma_D \rightarrow_{\omega \rightarrow 0} \Delta^2/\omega$ (leading to a gap in the spectrum). In the heterostructures we study, we find that outside the high density region, correlations are weak ($Z \approx 1$), and that as one moves to the interior of thicker heterostructures, correlations increase (Z decreases). Mott

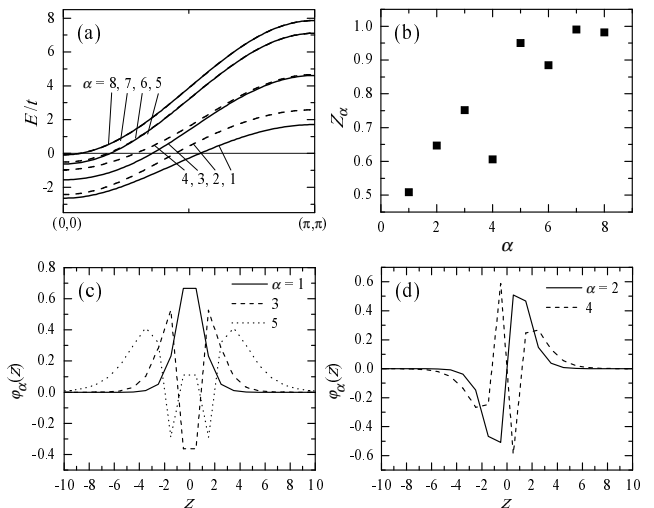


FIG. 3: (a) Dispersion relations of filled-subband quasi particles calculated for 3 layer heterostructure with $U = 16t$ and $\varepsilon = 15$. Solid and broken lines are for odd- and even- α , respectively. (b) Subband quasiparticle weights. (c, d) Quasiparticle wave functions for $\alpha = 1, 3, 5$ and $2, 4$ at $\omega = 0$. Here the heterostructure is defined by +1 charges placed at $z = 0, \pm 1$ so the electronic (B) sites are at half integer values of z .

insulating solutions ($Z = 0$) are never found; instead $\Sigma_D(z, \omega) \sim [1 - Z^{-1}(z)]\omega$ with $0 < Z < 1$ for all layers z , although in the interior of thick, large U heterostructures Z is only nonvanishing because of leakage (quantum tunneling) of quasiparticles from the edges, and goes exponentially towards zero.

The nonvanishing Z indicates a Fermi liquid state with well defined coherent quasiparticles (thus negligible low frequency scattering). In the heterostructure context the quasiparticles form subbands, with quasiparticle energies $E_\alpha(k_{\parallel})$ and wave functions $\varphi_\alpha(z; E_\alpha(\vec{k}_{\parallel}))$ which are the low energy eigenfunctions and eigenvalues of

$$\left[Z^{-1}(z)E_\alpha \delta_{z,z'} + \mu - H_{band}(\vec{k}_{\parallel}) - H_{Coul} \right] \varphi_\alpha(z') = 0. \quad (8)$$

(We note that the 2-site DMFT method used here is believed to give reasonable results for Z but of course neglects scattering effects. Near $E_\alpha = 0$ scattering is unimportant but of course will increase at higher energies.)

Numerical results for the coherent quasiparticles in a heterostructure with $n = 3$ and $U = 16t$ are shown in Fig. 3. For these parameters we find 8 quasiparticle bands with non-vanishing electron density. The calculated dispersion relations are shown in panel (a) and are labelled $\alpha = 1 \dots 8$ in order of decreasing electron density. We observe that the band splittings depend on momentum because of the layer dependence of Z . The corresponding quasiparticle weights Z_α and real-space wave functions $\varphi_\alpha(z)$ at $\omega = 0$ are shown in Fig. 3(b) and (c,d), respectively. (These quantities vary somewhat over

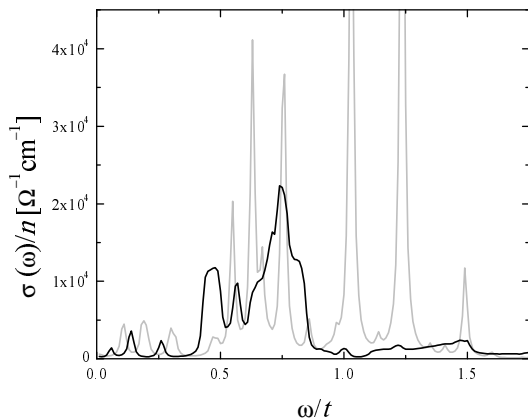


FIG. 4: Heavy lines: low frequency (quasiparticle-region) optical conductivity for $n = 3$, $U = 16t$ heterostructure. Peaks arise from transition among subbands shown in Fig. 3(a). Light lines: conductivity calculated from Hartree-Fock approximation to same Hamiltonian.

the band also). Z_α is the smallest for the $\alpha = 1$ subband because its real-space wave function contains the largest weight at $z = \pm 0.5$, where the charge density is the largest and, therefore, the correlation effect is the strongest [see Fig. 3(c)]. Z_α generally increases with increasing α , because as α increases the wave function amplitudes $|\varphi_\alpha(z)|$ decrease in the high density regions (near $z = 0$). The anomalies observed in Z_α at $\alpha = 4, 6$ correspond to the increase of $|\varphi_\alpha(z = \pm 0.5)|$ due to the symmetry of the wave function [see Fig. 3(d)].

The coherent subbands may be studied by optical conductivity with electric field directed along [001]. As an example, the heavy line in Fig. 4 shows the quasiparticle contribution to the conductivity spectrum, calculated for a heterostructure with $n = 3$ and $U = 16t$ using the standard Kubo formula with optical matrix element obtained by applying the Peierls phase ansatz to H_{band} (and $t = 0.3$ eV). Three main features are evident at $\omega = 0.75t, 0.55t$ and $0.45t$; each of these has contributions from two interband transitions, ($1 \rightarrow 2, 2 \rightarrow 3$), ($3 \rightarrow 4, 4 \rightarrow 5$) and ($5 \rightarrow 8, 6 \rightarrow 7$) respectively. The optical features are not sharp because the quasiparticle band splitting depends on \vec{k}_\parallel . The weaker features at lower energies arise from transitions involving high-lying, only slightly occupied bands. The lighter lines in Fig. 4 show the optical conductivity computed using the Hartree-Fock approximation. We see that the spectra are qualitatively similar, but that the Hartree-Fock absorption features occur at a larger energy because the Z -induced band narrowing is absent and are delta functions because in the Hartree-Fock approximation the subbands splittings are \vec{k}_\parallel -independent.

To summarize, we have presented the first dynamical mean field study of a ‘correlated electron heterostructure’, in which the behavior is controlled by the spreading of the electronic charge out of the confinement region.

Our results show how the electronic behavior evolves from the weakly correlated to the strongly correlated regions, and in particular confirms the existence of an approximately three unit cell wide crossover region in which a system, insulating in bulk, can sustain metallic behavior. We found that even in the presence of very strong bulk correlations, the metallic edge behavior displays a finite (roughly factor-of-two-to-three) mass renormalization. We showed how the magnitude of the renormalization is affected by the spatial structure of the quasiparticle wave function and determined how this renormalization affects physical properties, in particular the optical conductivity. Important future directions for research is to examine the phase diagram, using beyond Hartree-Fock techniques, and to generalize the results presented here to more complicated and realistic cases.

We acknowledge very fruitful discussions with M. Potthoff and H. Monien. This research was supported by NSF DMR-00081075 (A.J.M.) and the JSPS (S.O.).

-
- [1] M. Imada, A. Fujimori, and Y. Tokura, Rev. Mod. Phys. **70**, 1039 (1998).
 - [2] Y. Tokura and N. Nagaosa, Science **288**, 462 (2000).
 - [3] C.H. Ahn, S. Gariglio, P. Paruch, T. Tybell, L. Antognazza, J.-M. Triscone, Science, **284**, 1152 (1999).
 - [4] S. Gariglio, C.H. Ahn, D. Matthey, J.-M. Triscone, Phys. Rev. Lett. **88**, 067002 (2002).
 - [5] A. Ohtomo, D. A. Muller, J. L. Grazul, and H. Y. Hwang, Nature **419**, 378 (2002).
 - [6] M. Izumi, Y. Ogimoto, Y. Konishi, T. Manako, M. Kawasaki and Y. Tokura, Mat. Sci. Eng. B **84**, 53 (2001) and references therein.
 - [7] A. Biswas, M. Rajeswari, R. C. Srivastava, Y. H. Li, T. Venkatesan, R. L. Greene and A. J. Millis, Phys. Rev. B **61**, 9665 (2000).
 - [8] A. Biswas, M. Rajeswari, R. C. Srivastava, T. Venkatesan, R. L. Greene, Q. Lu, A. L. deLozanne, and A. J. Millis, Phys. Rev. B **63**, 184424 (2001).
 - [9] Z. Fang, I. V. Solovyev, and K. Terakura Phys. Rev. Lett. **84**, 3169 (2000).
 - [10] R. Matzdorf *et al.*, Science **289**, 746 (2000); R. G. Moore, J. Zhang, S. V. Kalinin, Ismail, A. P. Baddorf, R. Jin, D. G. Mandrus, and E. W. Plummer, Phys. Stat. Sol. in press (2004).
 - [11] M. Potthoff and W. Nolting Phys. Rev. B **60**, 7834 (1999).
 - [12] S. Schwieger, M. Potthoff, and W. Nolting, Phys. Rev. B **67**, 165408 (2003).
 - [13] S. Okamoto and A. J. Millis, Nature **428**, 630 (2004).
 - [14] S. Okamoto and A. J. Millis, cond-mat/0404275 (Phys. Rev. B (in press)).
 - [15] A. Georges, B. G. Kotliar, W. Krauth and M. J. Rozenberg, Rev. Mod. Phys., **68**, 13 (1996).
 - [16] M. Potthoff, Phys. Rev. B **64**, 165114 (2001).
 - [17] S. Okamoto and A. J. Millis, unpublished.
 - [18] M. Ulmke, Eur. Phys. J. B **1**, 301 (1998).